Donor/acceptor type photodetectors: Role of substitution in acceptor material

Satyajit Sahu and Amlan J. Pal

Citation: Journal of Applied Physics **99**, 114503 (2006); doi: 10.1063/1.2199348
View online: http://dx.doi.org/10.1063/1.2199348
View Table of Contents: http://scitation.aip.org/content/aip/journal/jap/99/11?ver=pdfcov
Published by the AIP Publishing

Donor/acceptor type photodetectors: Role of substitution in acceptor material

Satyajit Sahu and Amlan J. Pal[a)]
Indian Association for the Cultivation of Science, Department of Solid State Physics, Jadavpur, Kolkata 700032, India

(Received 18 October 2005; accepted 1 March 2006; published online 2 June 2006)

We report fabrication and characterization of photodetectors based on organic semiconductors. Single and multiple heterostructures between electron donor and acceptor materials are used. Moreover, by varying the substitutes of the acceptor molecule, five different donor/acceptor combinations are presented. Photocurrent depends on the choice of the acceptor material, showing importance of energy mismatch between lowest unoccupied molecular orbital (and highest occupied molecular orbital) levels of donor and acceptor molecules. Additionally, the photocurrent also depends on the number of donor/acceptor interfaces. The results can be explained in terms of an energy band diagram of the devices. From the impedance spectroscopy, we show that the change in dielectric constant of the active material due to illumination has a direct relevance to the external current of the photodetectors. © 2006 American Institute of Physics. © *2006 American Institute of Physics*. [DOI: 10.1063/1.2199348]

I. INTRODUCTION

In recent years, organic semiconductors have played key roles in different electronic and optoelectronic devices. In most of the devices, the selection of suitable materials and the device architectures are the key parameters. In general, heterostructures between electron and hole transporting layers or electron donor and acceptor materials are used in the devices. Photodetectors, along with light-emitting diodes based on organic semiconductors, can be integrated for communication devices and displays. In photodetectors based on electron donor and acceptor materials,[1–4] excitons are photogenerated in the bulk of the devices. They dissociate into electrons and holes at donor/acceptor (D/A) interfaces. Under bias, the carriers are transported to the opposite electrodes to result in photocurrent in the external circuit. Donor and acceptor materials are chosen in such a way that under a reverse bias, the contacts with the electrodes act as blocking in nature. Hence, under dark conditions, little or no current flows through the device, so that even a weak light can be detected. In addition, molecular orbitals of the materials should be such that the difference between lowest unoccupied molecular orbitals (LUMO) of the acceptor and the donor is more than the binding energy of the excitons generated in the donors. Similarly, for excitons generated in an acceptor, the difference between the highest occupied molecular orbitals (HOMO) of the respective components overcomes the exciton binding energy. Additionally, the number of D/A interfaces determines exciton-dissociating volume.[5–7] The interfaces, however, also induce energy barriers for electron and hole transport in the device. Hence, apart from the electrode work functions and electrochemical properties of the active materials, device architecture has to be optimized in a photodetector.

In this work, we have chosen a series of electron accepting fluorone molecules in which the electrochemical properties have been tuned by different substitutes. We have fabricated and characterized photodetectors based on the fluorone molecules in association with an electron donor material, so that the role of the acceptor's molecular orbitals on photocurrent can be studied.

II. EXPERIMENT

In the present work, copper(II) phthalocyanine-3,4′,4″,4‴-tetrasulfonic acid and five fluorone dyes in the xanthene class were used as donor and acceptor materials, respectively. To deposit layer-by-layer (LbL) films via electrostatic self-assembly,[8,9] sodium salts of the dyes and poly(allylaminehydrochloride) (PAH) were used as anions and polycation, respectively. The molecular structures of the fluorone dyes are shown in the inset of Fig. 1. With different halogen substitutes, we had Fluorescein Sodium, Erythrosin B, Eosin Y, Phloxine B, and Rose Bengal as acceptor materials. The devices were fabricated on indium tin oxide (ITO) coated glass substrates. To deposit LbL films, ITO coated substrates were first dipped in a 5×10^{-3} M dye solution (pH=6.8) for 15 min. The substrates were washed thrice by dipping in deionized water baths for 2, 2, and 1 min. They were then immersed in a PAH bath, which had a concentration of 5×10^{-3} M (pH=6.8), followed by the same rinsing protocol. This resulted in one LbL layer of a dye molecule. Heterostructures between donor and different acceptor materials were deposited. All the devices contained 15 layers of donor and acceptor each. In effect, we introduced one and four D/A interfaces in the molecular scale by depositing $D_{11}/(D/A)_4/A_{11}$ and D_{15}/A_{15} films for all of the five acceptor materials. Here D and A represent donor and acceptor monolayers, respectively. The films were annealed in a vacuum oven at 110 °C for 6 *h*. Total thickness of the films was 70 nm. To complete device fabrication, aluminum (Al)

a)Electronic mail: sspajp@iacs.res.in

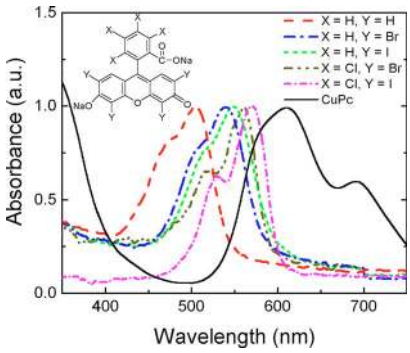

FIG. 1. (Color online) Electronic absorption spectra of the dyes used in fabricating the devices. The spectra have been normalized to unity at the peak wavelength. The spectra from left to right represent Fluorescein Sodium, Eosin Y, Erythrosin B, Phloxine B, Rose Bengal, and Copper Phthalocyanine, respectively. Inset shows molecular structure of the fluorone dyes.

was deposited on top of the film by thermal evaporation in vacuum below 10^{-5} Torr. Shadow masks determined the device's area, which were about 5.5 mm^2.

Electronic absorption spectra of the LbL films of CuPc and the acceptor dyes, deposited on quartz substrates, were recorded by a Hewlett Packard UV-Vis spectrophotometer HP-8453. Device characterization was carried out in a shielded vacuum chamber with an optical window. Current-voltage (*I-V*) characteristics were recorded under dark and illumination conditions. Intensity of white light (xenon lamp) was varied in the 10–100 mW/cm^2 range by using neutral density filters. A Yokogawa 7651 dc source and a Keithley 486 picoammeter were used for the *I-V* measurements. Voltage step was 0.05 V with a scan rate of 5 mV/s. To avoid any displacement current, voltage was scanned to both directions and current values were averaged. Impedance spectroscopy was carried out by a Solartron 1260A impedance analyzer in the 1 Hz–12 MHz range with a test voltage of 100 mV rms.

III. RESULTS AND DISCUSSION

A. Electronic absorption spectra

The absorption spectra of CuPc and fluorone dyes are shown in Fig. 1. The spectra show the range over which each of the D/A combinations would remain sensitive. The halogens, which act as electron-accepting groups in the fluorone dye, are known to decrease electron affinity or LUMO and ionization potential or HOMO of the organics. Since CuPc's HOMO and LUMO are higher than the respective levels of any of the fluorone dyes, the halogen groups would provide a higher mismatch in the HOMO (and LUMO) levels at the interface between the donor and acceptor materials. Figure 1 shows that with addition of halogen groups, the absorption spectra shift towards the long-wavelength region. The red-shift of the spectra shows that in addition to the decrease in HOMO and LUMO levels, the halogen groups lower the band gap of the dyes. Hence, the energy mismatch of the LUMO levels at the D/A interfaces will be higher as compared to the mismatch of the HOMO levels. For each of the acceptor cases, the spectrum from a $D_{11}/(D/A)_4/A_{11}$ film

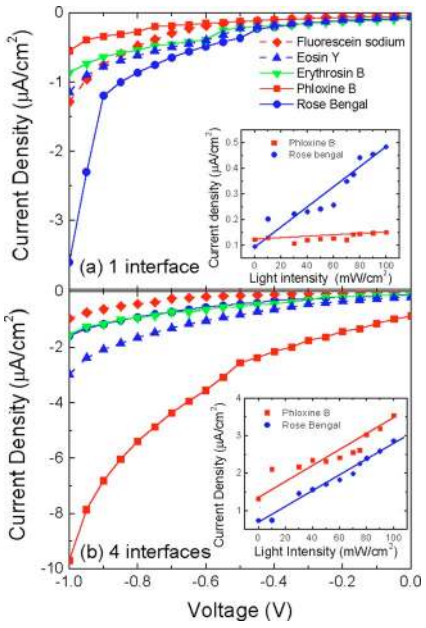

FIG. 2. (Color online) Current-voltage plot under 100 mW/cm^2 white light illumination of devices based on CuPc and different acceptor molecules. The device structures were (a) $ITO/D_{15}/A_{15}/Al$ and (b) $ITO/D_{11}(D/A)_4/A_{11}/Al$, where D and A represents one LbL layer of CuPc and acceptor molecule, respectively. Different acceptor molecules, as represented by different symbols, are indicated as legends. The insets show light intensity dependence of photocurrent at −0.6 V for the Rose Bengal and Phloxine B cases. The straight lines are best fits to the points in each of the cases.

were algebraic sums of the spectra of the individual components. This showed that charge-transfer complex did not form at the D/A interfaces. Also, the energy offset between the HOMO or LUMO levels of the donor and any of the acceptor molecules is more than the exciton binding energy (~0.2 eV). Hence, the CuPc and fluorone dyes formed suitable combinations to act as photodetectors.

B. Current-voltage characteristics

We have fabricated device with one and four D/A interfaces. In photodetectors, excitons are inherently dissociated due to the applied bias. In addition, D/A interfaces with energy mismatch in LUMO (and HOMO) levels of the individual components act as dissociating centers. Hence, the devices with four D/A interfaces should favor exciton dissociation. Figures 2(a) and 2(b) show reverse bias section of *I-V* characteristics from devices under 100 mW/cm^2 illumination. Devices with five different acceptor materials and two different architectures, namely one and four D/A interfaces, are represented in the figures.

The *I-V* characteristics show that all the devices responded to illumination and gave rise to photocurrent. The figures show that the photocurrent response was in general higher in the four-interface case. The photocurrent depended on (1) the number of D/A interfaces and (2) the substitutes of the acceptor material. The dependence with the substitutes again differed in one and four D/A interface cases. That is, for example, Rose Bengal as an acceptor in a D_{15}/A_{15} device yielded the highest photocurrent, while in the $D_{11}/(D/A)_4/A_{11}$ case, the Phloxine B based device provided

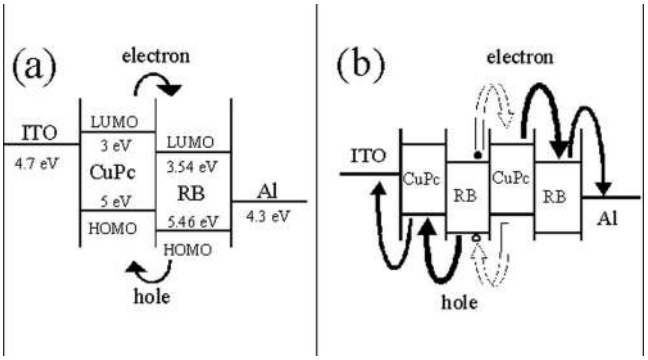

FIG. 3. A schematic representation of energy band diagram of (a) ITO/D_{15}/A_{15}/Al and (b) ITO/D_{11}/$(D/A)_4$/A_{11}/Al structures with CuPc and Rose Bengal (RB) as donor and acceptor material, respectively. Open arrows represent barriers for carrier transport. In (b), only two D/A interfaces have been represented for simplicity.

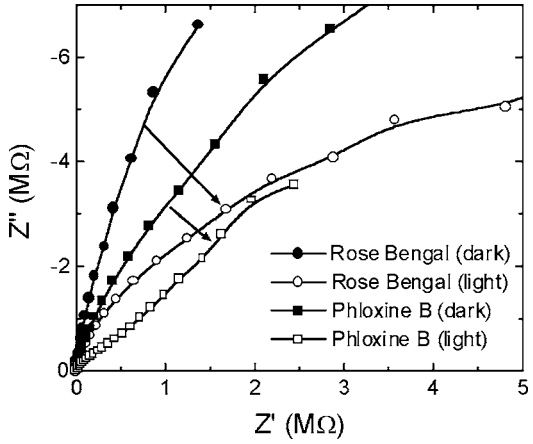

FIG. 4. Cole-Cole plots for ITO/D_{11}/$(D/A)_4$/A_{11}/Al devices in dark and under 100 mW/cm^2 illumination conditions. Results for Rose Bengal and Phloxine B as acceptor molecules are shown.

more photocurrent than that with other acceptors. The results therefore show the importance of electrochemical properties of the individual components and exciton dissociating volume in organic photodetectors.

The role of substitutes in the acceptor molecule on photocurrent is itself of interest and can be understood in terms of energy band diagrams. Schematic diagrams for the D_{15}/A_{15} and $D_{11}/(D/A)_4/A_{11}$ devices are represented in Figs. 3(a) and 3(b), respectively. The band diagram clearly shows the energy difference between HOMO (and also LUMO) levels in the system that provides the required energy for exciton dissociation. In addition, the diagram for the four-interface case shows the barriers that an electron or a hole would face during transport to the opposite electrode.

With the addition of halogens, the decrease in LUMO was more as compared to that of the HOMO. Hence, the energy mismatch of LUMO levels would be more than the mismatch of the HOMO levels at the D/A interface. Since light was illuminated through the ITO electrode to the donor side, most of the excitons would form at the donor molecules. Hence, electron transfer from the LUMO of donor to acceptor would be the key process. For excitons generated at the acceptor molecule, transfer of holes from the HOMO of acceptor to the donor would have some contribution. Therefore, the energy mismatch of the LUMO levels would be more relevant than that of the HOMO levels. In other words, a higher number of halogen substitutes (e.g., Rose Bengal, Phloxine B) would increase the possibility of exciton dissociation in the donor material.

Carrier transport would also play a major role in the photodetectors, especially in devices with only one interface. Mobility of the carriers through the donor and acceptor layers, or their conductivity levels, would determine the effective photocurrent in the external circuit. In other words, two factors—namely, (1) the energy mismatch of the LUMO (and also HOMO) levels at the D/A interface and (2) the conductivity of donor and acceptor materials—would determine the photocurrent. The results in Fig. 2(a) show that Rose Bengal as an acceptor, which offers the highest mismatch in LUMO levels with CuPc and has a moderately high level of conductivity, yielded the highest photocurrent as compared to devices based on other acceptor materials.

In devices with four interfaces, apart from the above-mentioned factors, energy barriers at the interfaces play an additional role. That is, the mismatch of LUMO levels at the D/A interface acts as a barrier for electron transport. Similarly, the mismatch in HOMO levels causes barriers for hole transport. Hence, the difference in LUMO, which favored exciton dissociation in the one interface case [Fig. 2(a)], would have opposing contribution in photocurrent [Fig. 2(b)]. That is, in devices with four interfaces, a higher difference in LUMO levels (1) favors exciton dissociation but (2) offers energy barriers for carrier transport. A combined effect of the factors has resulted in the highest photocurrent in devices based on Phloxine B as acceptor material as compared to other cases.

We have studied *I-V* characteristics of the devices under different illumination intensities. Device current at any voltage increased linearly with light intensity. In the insets of Figs. 2(a) and 2(b), we plot device current at −0.6 V as a function of light intensity for the D_{15}/A_{15} and $D_{11}/(D/A)_4/A_{11}$ devices, respectively, with Rose Bengal and Phloxine B as acceptor material. In devices based on one interface, the plots show a sublinear slope. In such devices, since the excitons generated only close to the interface can be dissociated, an increase in light intensity did not amplify the photocurrent linearly. In the four-interfaces case, the plots exhibit a slope of unity with dark current as the intercept with the *y* axis. In such devices, excitons generated over a large volume can be dissociated. Such a linear behavior is ideal for a photodetector. The results hence show that the CuPc/Fluorone combination with multiple interfaces can suitably be used in photodetectors.

C. Dielectric spectroscopy

To study the relative effect of (1) exciton dissociation, (2) transport of carriers, and (3) energy barriers in these devices, we have studied impedance spectroscopy of the devices. Measurements were carried out in dark and illumination conditions for devices with different acceptor groups and also for one and four D/A interfaces. Plots between real and imaginary components of complex impedance, namely

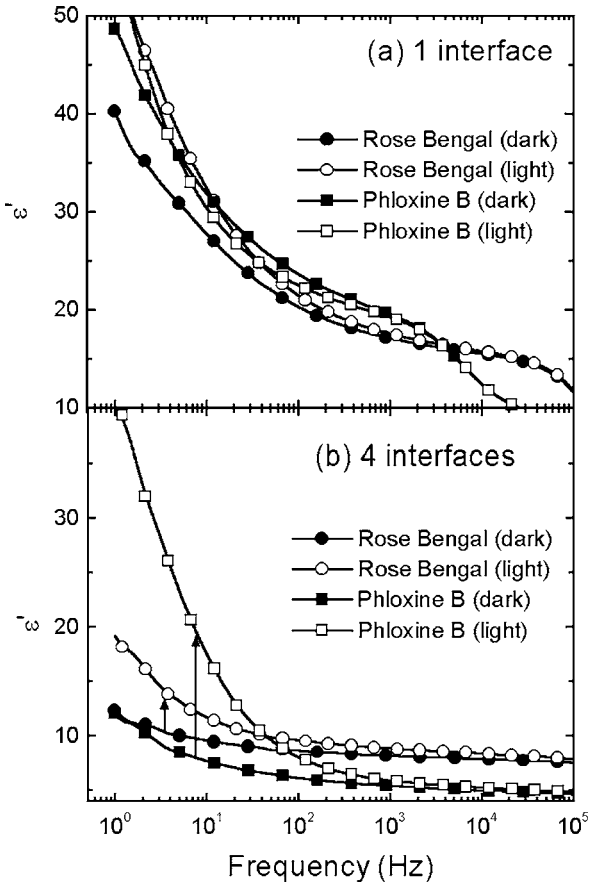

FIG. 5. Relative dielectric constant vs frequency plot for (a) ITO/D_{15}/A_{15}/Al and (b) ITO/D_{11}/$(D/A)_4$/A_{11}/Al devices in dark and under 100 mW/cm^2 illumination conditions. Results for Rose Bengal and Phloxine B as acceptor molecule are shown.

Cole-Cole plots, for all the devices showed signs of semicircles. In each of the cases, the radius in Cole-Cole plots, representing bulk resistance of the device, decreased when the device was illuminated. Results from Rose Bengal and Phloxine B based devices are shown in Fig. 4. The decrease in bulk resistance of the device could be due to the increase in carrier mobility. The dissociated excitons may increase the carrier concentration in the device resulting in an increase in the mobility of the charge carriers.

From the impedance spectroscopy, we calculated relative dielectric constant (ε') of the active material in dark and illumination conditions. ε' should be sensitive to exciton dissociation or charge separation and carrier confinement in the devices. In Figs. 5(a) and 5(b), we show ε'-frequency plots for the one- and four-interface cases, respectively. The results are presented for devices with Rose Bengal and Phloxine B in dark and illumination conditions. The figures show that ε' of the active material responded to the incident light. In fact, ε' increased with illumination. In the case for one interface, Fig. 5(a), the change in ε' was highest in devices with Rose Bengal. On the other hand, Fig. 5(b) for four interfaces shows that the increase in ε' was much more for the Phloxine B case. Hence, the change in ε' has a direct correspondence with the photocurrent response, as shown in Figs. 3(a) and 3(b).

IV. CONCLUSION

In conclusion, we have fabricated photodetectors based on copper phthalocyanine and fluorone, which acted as donor and acceptor materials. Substitutes of fluorone were varied to tune their electron-accepting properties. The device current of the photodetector under illumination depended on the (1) acceptor molecule, (2) number of donor/acceptor interfaces, and (3) charge transporting regions. The results were explained in terms of a band diagram by considering energy mismatch of LUMO (and also HOMO) levels of the donor and acceptor molecules and exciton dissociation volume into account. Additionally, dielectric properties of the active material in dark and under illumination condition showed that the change in relative dielectric constant had a direct correspondence with the photocurrent of the device.

ACKNOWLEDGMENTS

S.S. acknowledges support from CSIR. The authors also acknowledge financial support from the Council of Scientific and Industrial Research through Project No. 03(1044)/05/EMR-II.

[1]P. Peumans, A. Yakimov, and S. R. Forrest, J. Appl. Phys. **93**, 3693 (2003).
[2]Y. Ohmori, H. Kajii, M. Kaneko, K. Yoshino, M. Ozaki, A. Fujii, M. Takenaka, and T. Taneda, IEEE J. Sel. Top. Quantum Electron. **10**, 70 (2004).
[3]D. Natali, M. Sampietro, M. Arca, C. Denotti, and F. A. Devillanova, Synth. Met. **137**, 1489 (2003).
[4]P. Schilinsky, C. Waldauf, and C. J. Brabec, Appl. Phys. Lett. **81**, 3885 (2002).
[5]M. F. Durstock, R. J. Spry, J. W. Baur, B. E. Taylor, and L. Y. Chiang, J. Appl. Phys. **94**, 3253 (2003).
[6]H. Mattoussi, M. F. Rubner, F. Zhou, J. Kumar, S. K. Tripathy, and L. Y. Chiang, Appl. Phys. Lett. **77**, 1540 (2000).
[7]B. Pradhan, A. Bandyopadhyay, and A. J. Pal, Appl. Phys. Lett. **85**, 663 (2004).
[8]G. Decher, Science **277**, 1232 (1997).
[9]S. S. Shiratori and M. F. Rubner, Macromolecules **33**, 4213 (2000).